



The Protective Effect of Aspirin Eugenol Ester on Paraquat-Induced Acute Liver Injury Rats

Zhen-Dong Zhang, Ya-Jun Yang, Xi-Wang Liu, Zhe Qin, Shi-Hong Li and Jian-Yong Li*

Key Lab of New Animal Drug Project of Gansu Province, Key Lab of Veterinary Pharmaceutical Development of Ministry of Agriculture and Rural Affairs, Lanzhou Institute of Husbandry and Pharmaceutical Sciences of CAAS, Lanzhou, China

Aspirin eugenol ester (AEE) possesses anti-inflammatory and anti-oxidative effects. The study was conducted to evaluate the protective effect of AEE on paraquat-induced acute liver injury (ALI) in rats. AEE was against ALI by decreasing alanine transaminase and aspartate transaminase levels in blood, increasing superoxide dismutase, catalase, and glutathione peroxidase levels, and decreasing malondialdehyde levels in blood and liver. A total of 32 metabolites were identified as biomarkers by using metabolite analysis of liver homogenate based on ultra-performance liquid chromatography-tandem mass spectrometry, which belonged to purine metabolism, phenylalanine, tyrosine and tryptophan biosynthesis, glycerophospholipid metabolism, primary bile acid biosynthesis, aminoacyl-tRNA biosynthesis, phenylalanine metabolism, histidine metabolism, pantothenate, and CoA biosynthesis, ether lipid metabolism, beta-Alanine metabolism, lysine degradation, cysteine, and methionine metabolism. Western blotting analyses showed that Bax, cytochrome C, caspase-3, caspase-9, and apoptosis-inducing factor expression levels were obviously decreased, whereas Bcl-2 expression levels obviously increased after AEE treatment. AEE exhibited protective effects on PQ-induced ALI, and the underlying mechanism is correlated with antioxidants that regulate amino acid, phospholipid and energy metabolism metabolic pathway disorders and alleviate liver mitochondria apoptosis.

Keywords: aspirin eugenol ester, paraquat, metabolites, hepatotoxicity, antioxidation

OPEN ACCESS

Edited by:

Jianpeng Sheng,
Nanyang Technological
University, Singapore

Reviewed by:

Haijun Li,
Jilin University, China
Wei Li,
Jilin University, China

*Correspondence:

Jian-Yong Li
lijy1971@163.com

Specialty section:

This article was submitted to
Gastroenterology,
a section of the journal
Frontiers in Medicine

Received: 30 July 2020

Accepted: 30 November 2020

Published: 17 December 2020

Citation:

Zhang Z-D, Yang Y-J, Liu X-W, Qin Z,
Li S-H and Li J-Y (2020) The
Protective Effect of Aspirin Eugenol
Ester on Paraquat-Induced Acute
Liver Injury Rats.
Front. Med. 7:589011.
doi: 10.3389/fmed.2020.589011

INTRODUCTION

PQ is a non-selective herbicide with excellent effect, which has been widely used in the world for many years (1–3). PQ is extremely toxic to humans (4, 5). Studies have shown that when taking about 10 ml PQ, patients can die of multiple organ failure a few hours later (6). The accumulation of PQ can damage the main organs such as lung, kidney, liver and heart (7). It is reported that the liver is one of the main target organs of PQ poisoning, which is often accompanied by the formation of free radicals (8, 9). The liver is the main metabolic and detoxifying organ of the human body (10, 11). A multiple potentially harmful stimuli challenge the liver, including free radicals. It is well known that drugs and other substances are further transformed and metabolized after being absorbed by the body, resulting in the production of free radicals in the liver. Excessive free radicals produce oxidative stress on the liver, which in turn leads to oxidative damage to the liver (12).

Currently, the molecular mechanism of hepatotoxicity induced by PQ is not completely understood. It is known that the redox response is one of the main factors involved in the toxic effects of PQ (13). It has been reported that PQ molecules can interfere with the electron transport chain and then inhibit the synthesis of NADPH (14). Excessive production of ROS was observed during PQ poisoning, indicating that oxidative stress was involved in the pathological changes induced by PQ. Excessive ROS and excessive free radicals lead to oxidative stress by destroying DNA, proteins and lipids (15). Therefore, the premise of the toxic effect of PQ is its induced oxidative stress. At present, the main methods for the treatment of PQ poisoning are immunosuppressant and hemodialysis (16). Existing clinical treatments for severe PQ poisoning only relieve symptoms (17). In recent decades, new drugs to treat the toxicity of PQ have been developed. In the early stages of poisoning, the use of antioxidants has been shown to effectively reduce the damage of PQ to organs. Therefore, it is imperative to develop potential effective drugs for the treatment of PQ poisoning.

AEE is a new potential pharmaceutical compound possessing anti-inflammatory and anti-oxidative stress pharmacological activity (18–22). The effect of AEE against H₂O₂-induced oxidative stress of human umbilical vein endothelial cells is consistent with the AEE-enhanced expression of Bcl-2 and Nrf2 (18, 23). It has been well documented that AEE could alleviate H₂O₂-induced dysfunction of mitochondria, the generation of ROS productions and the increase of apoptosis via enhancing the expression of Bcl-2 and Nrf2 (18, 23). It is well known that the dysfunction of mitochondria could release cytochrome C, apoptosis inducing factor (AIF), and other factor into cytoplasm to mediate downstream apoptotic signals causing cell apoptosis (24, 25), while the exacerbation of reactive oxygen species (ROS) induced by the dysfunction of mitochondria is also vital incentive of cell apoptosis (26, 27).

MATERIALS AND METHODS

Chemicals

AEE (99.5%) was prepared in Lanzhou Institute of Husbandry and Pharmaceutical Sciences of CAAS (Lanzhou, China). MS-grade acetonitrile was purchased from Thermo Fisher Scientific (Waltham, MA, USA). Formic Acid (98.0%, for LC-MS) was purchased from Tokyo Chemical Industry (Shanghai, China). Catalase assay kit was purchased from Solarbio (Beijing, China). Glutathione peroxidase (GPx), GSH and GSSG assay kit, superoxide dismutase (SOD), and malondialdehyde (MDA) assay kit were purchased from Beyotime (Shanghai, China). Caspase-3 assay kit was purchased from Jianglai Chemical Biotechnology (Shanghai, China). The antibodies of Caspase-9, Caspase-3, Bax, Bcl-2, Cyt C, AIF, and IgG were purchased from abcam (Shanghai, China). Alanine aminotransferase kit and aspartate aminotransferase kit were purchased from Mlbio (Shanghai, China).

Animal Experiment

Eighteen male specific pathogen-free SD rats (6 weeks old) weighing 120–130 g were purchased from the Laboratory Animal

Center of Lanzhou Veterinary Research Institute (Lanzhou, China). All animals were placed in groups in SPF-class housing of laboratory at a controlled relative humidity (55–65%), 12 h light/dark cycle and temperature (24 ± 2°C). The rats were randomly divided into three groups (*n* = 6): (1) control group, in which rats were administrated equivalent saline by intraperitoneal injection (ip); (2) PQ group, in which rats were administrated PQ (20 mg/kg body weight, ip) (28–30); (3) AEE groups, in which rats were pre-administrated AEE (54 mg/kg/day body weight) by gavage once a day for 1 week before being administrated PQ. The rats in the different groups were sacrificed after a single intraperitoneal injection of 20 mg/kg PQ for 24 h. All experimental protocols and procedures were approved by the Institutional Animal Care and Use Committee of Lanzhou Institute of Husbandry and Pharmaceutical Science of Chinese Academy of Agricultural Sciences (Approval No. NKMYD201907018; Approval Date: 18 July 2019). Animal welfare and experimental procedures were performed strictly in accordance with the Guidelines for the Care and Use of Laboratory Animals issued by the US National Institutes of Health.

Metabonomic Analysis

Hepatic Tissue Sample Preparation

The hepatic tissue samples were homogenized with ice-cold physiological saline (10%, wt%, 1 g tissue in 10 mL of physiological saline) in an Ultra Turrax tissue homogenizer. After vortex mixing for 3 min, the samples were centrifuged at 12,000 rpm for 10 min at 4°C. The supernatant was subsequently analyzed by UPLC-QTOF-MS/MS.

UPLC-QTOF-MS/MS Conditions

Liquid chromatography was executed on DAD 1290 UPLC system (Agilent Technologies Inc., California, USA). Separation was performed on an Agilent SB C18 RRHD Column (2.1 × 150 mm, 1.8 μm). The temperature of the column was set to 35°C. Injection volume was 3 μL and autosampler temperature was set at 4°C. Mobile phase A consisted of water containing 0.1% formic acid and mobile phase B was acetonitrile containing 0.1% formic acid at a flow rate of 0.3 mL/min. The gradient elution of A was as follows: 98%A from 0 to 2 min, 98–55% A from 2 to 9 min, 55–30% A from 9 to 15 min, 30–2% A from 15 to 22 min, 2% A from 22 to 23 min, 2–98% A from 23 to 24 min and held at 98% A from 24 to 27 min. The mass spectrometer was operated in both positive and negative ionization modes. The fragment voltage was set to 135V and the skimmer voltage was set to 65 V. In positive ion mode, capillary voltage was 4.0 KV, while in negative ion mode, it was 3.5 KV. The temperature and the flow of the drying gas were 350°C and 10 L/min, respectively. The nebulizer pressure was set to 45 psig. Ions were scanned over a region of 50–1000 m/z.

Metabolomics Data Analysis

The raw MS data were initially processed with the Mass Profiler Professional (MPP) software (Agilent Technologies, USA) to filter noise, correct the baseline, align peaks, and identify and quantify peaks. The match tolerance of mass span is 10 ppm,

and the match tolerance of retention time's span is 0.10 min. The obtained data were imported into SIMCA-P (version 13.0, Umetrics AB, Umea, Sweden), where a principal component analysis (PCA) and partial least squares discriminant analysis (OPLS-DA) were performed on the dataset. The quality of OPLS-DA models was described by R^2X , R^2Y , and Q^2 , and its validity was evaluated by performing permutation testing (with 200 permutations). The variable importance in the projection (VIP > 1) value of the validated OPLS-DA model and the p values from one-way ANOVA ($p < 0.05$) were used as the measurement indices to select potential metabolites. Metabolites were identified through a mass-based search followed by manual verification. Accurate mass values of the molecular ions of interest in TOF-MS data were searched against METLIN and Human Metabolome Database (HMDB). Then, an MS/MS analysis was conducted to confirm the structure of potential biomarkers by matching the masses of the fragments. The parent ion mass tolerance is ± 10 ppm and mass/charge (m/z) of products tolerance is ± 10 ppm. The clustering analysis of the potential biomarkers and pathway analysis were performed using MetaboAnalyst 4.0 and the metabolic pathways were identified using the KEGG database.

Histopathology

Liver specimens were fixed with 10% formaldehyde. After fixation, the liver tissue was embedded in paraffin wax, sectioned to a thickness of 5 μ m and stained with hematoxylin-eosin staining.

Analysis of MDA, SOD, Caspase-3, GSH/GSSH, and GPx

The levels of MDA, SOD and the activity of caspase-3, the ratio of GSH/GSSH and GPx in the rat serum were assessed using the corresponding commercial kits according to the manufacturer's protocols.

Protein Expression Analysis

The expression of AIF, Bax, Bcl-2, Caspase-3, Caspase-9, and Cyt c among different treatment was assessed by Western blot analysis. In brief, total protein of the liver was extracted using RIPA, quantified by bicinchoninic acid (BCA) method, and separated by precast SDS-PAGE Gel (15%, 4–20%). The separated proteins were transferred onto polyvinylidene fluoride (PVDF) membrane using standard procedures. Blots were incubated with the primary antibody followed by horseradish peroxidase-conjugated secondary antibody. Results were detected using the G: Box Chemi XRQ Imaging System (Cambridge, UK).

RESULTS

AEE Reduces PQ-Induced Liver Injury in Rat

To verify whether AEE has a protective effect on PQ-induced hepatotoxicity *in vivo*, we explored the effect of AEE pretreatment on PQ-induced liver injury in rats. The results showed that PQ (20 mg/kg) could significantly cause liver tissue necrosis, cell atrophy and portal hyperemia in rats. Pretreatment with 54 mg/kg AEE for seven consecutive days by gavage markedly

attenuated the pathological injury of liver tissue induced by PQ (Figure 1). The results showed that AEE could effectively reduce the liver injury induced by PQ in rats.

AEE Attenuates PQ-Induced Oxidative Stress in the Liver of Rats

The results for CAT, MDA, SOD, GPx, and GSH/GSSH ratio in serum were shown in Figure 2. AEE significantly attenuated the increase in MDA and prevented the decrease in CAT, SOD, GPx activity, GSH/GSSH ratio caused by PQ in rats (Figure 2). These results suggested that AEE could effectively inhibit oxidative stress induced by PQ in rat liver.

Metabolomics Analysis of AEE Effect on PQ-Induced ALI in Rats

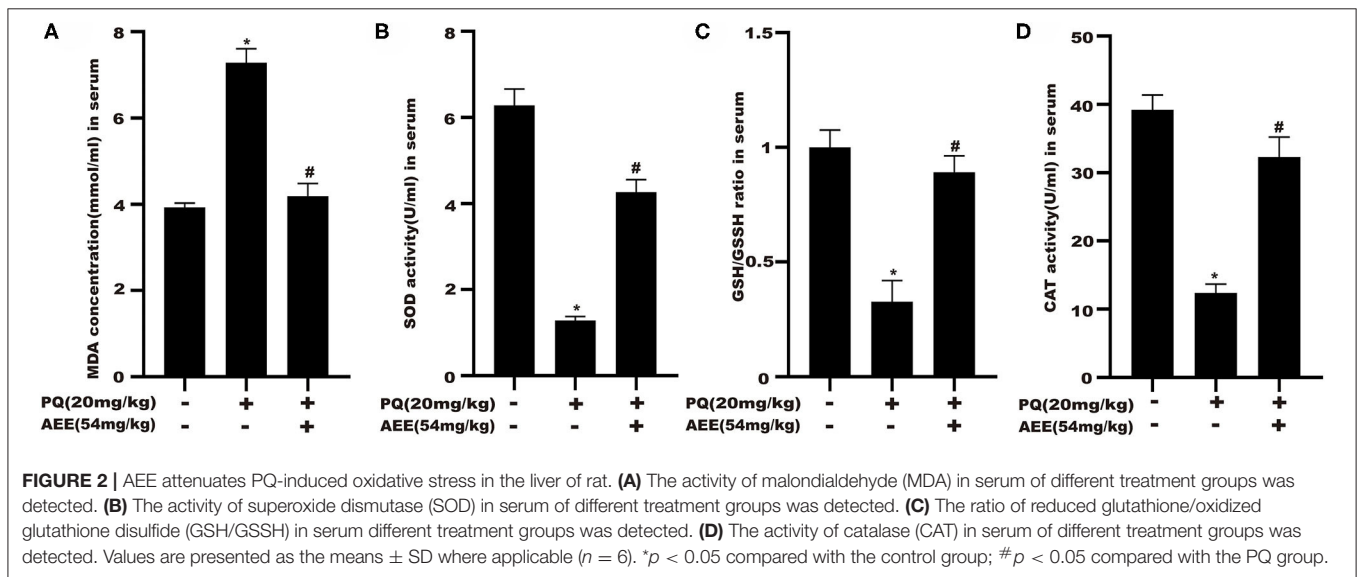
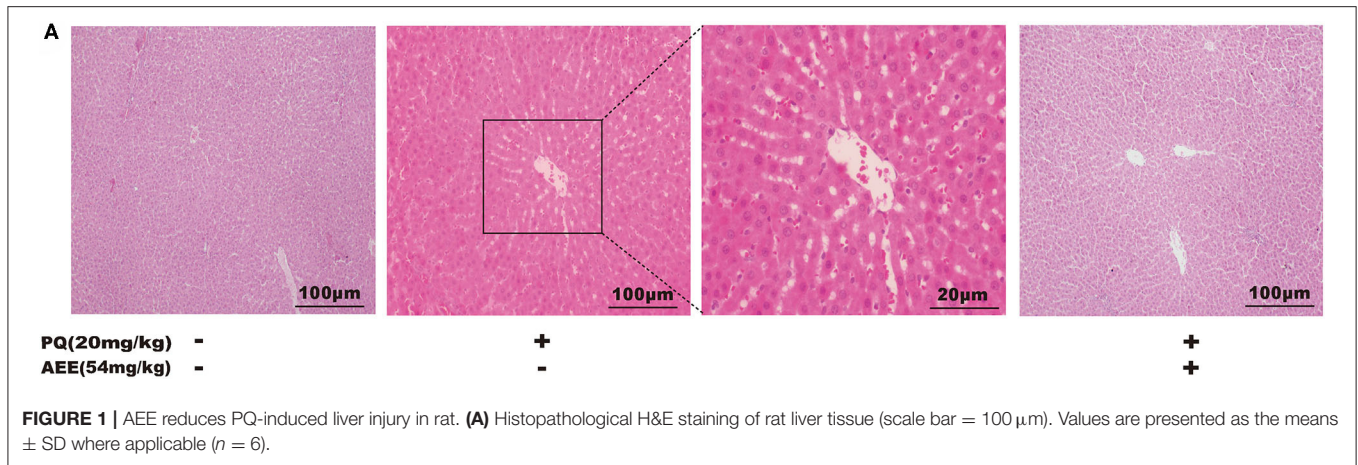
Analysis of Liver Metabolites

In this study, an unsupervised PCA was performed with the data from three experimental groups. In both positive and negative modes, the first two principal components explained 61.4 and 58.9% of the total variance, respectively. As shown in the PCA plots (Figures 3A,B,G,H), the three groups showed obvious separation in both positive and negative ion modes. In order to further maximize the separation and identification of metabolites, supervised orthogonal partial least squares discriminant analysis (OPLS-DA) was used. Then an OPLS-DA model was established between the PQ group and other groups to enhance the variation. The OPLS-DA score plots presented an obvious separation between the PQ group and other groups without any overlap in either the positive or negative modes (Figures 3C,E,I,K). The R^2X , R^2Y , and Q^2 values of the OPLS-DA model showed that the models were robust and had predictive abilities (Figures 3D,F,J,L).

Differential metabolites contributing to the separation were identified using variable importance in the projection (VIP) value and p value. The potential metabolites were screened with a VIP value > 1 and $p < 0.05$. As shown in Table 1, 32 metabolites were identified as potential metabolites, including dephospho-CoA, taurochenodesoxycholic acid, lysoPC(14:1), chenodeoxyglycocholic acid, PA(22:2), PA(22:2), cholic acid, 5,9,11-trihydroxyprosta-6E,14Z-dien-1-oate, lysoPE(18:2), lysoPE(20:4), lysoPE(16:0), lysoPC(16:0), L-Histidine, pipercolic acid, glycerophosphocholine, acetyl glycine, N-(2-Methylpropyl)acetamide, D-Asparagine, hypoxanthine, inosine, xanthosine, L-Phenylalanine, melatonin radical, ophthalmic acid, nonyl isovalerate, glutamylarginine, glutamylleucine, pipercolic acid, S-(PGJ2)-glutathione, L-Octanoylcarnitine, lysoPC(16:0), argininic acid, deoxycholic acid glycine conjugate, N-Undecanoylglycine. After AEE treatment, the levels of these metabolites normalized either due to upregulation or downregulation.

Metabolic Pathway Analysis

The related metabolic pathway analysis was performed on MetaboAnalyst 4.0. The metabolic pathway analysis data are shown as a bar chart and a bubble chart in Figure 4. There are 12 main metabolic pathways: purine metabolism, phenylalanine, tyrosine and tryptophan biosynthesis, glycerophospholipid



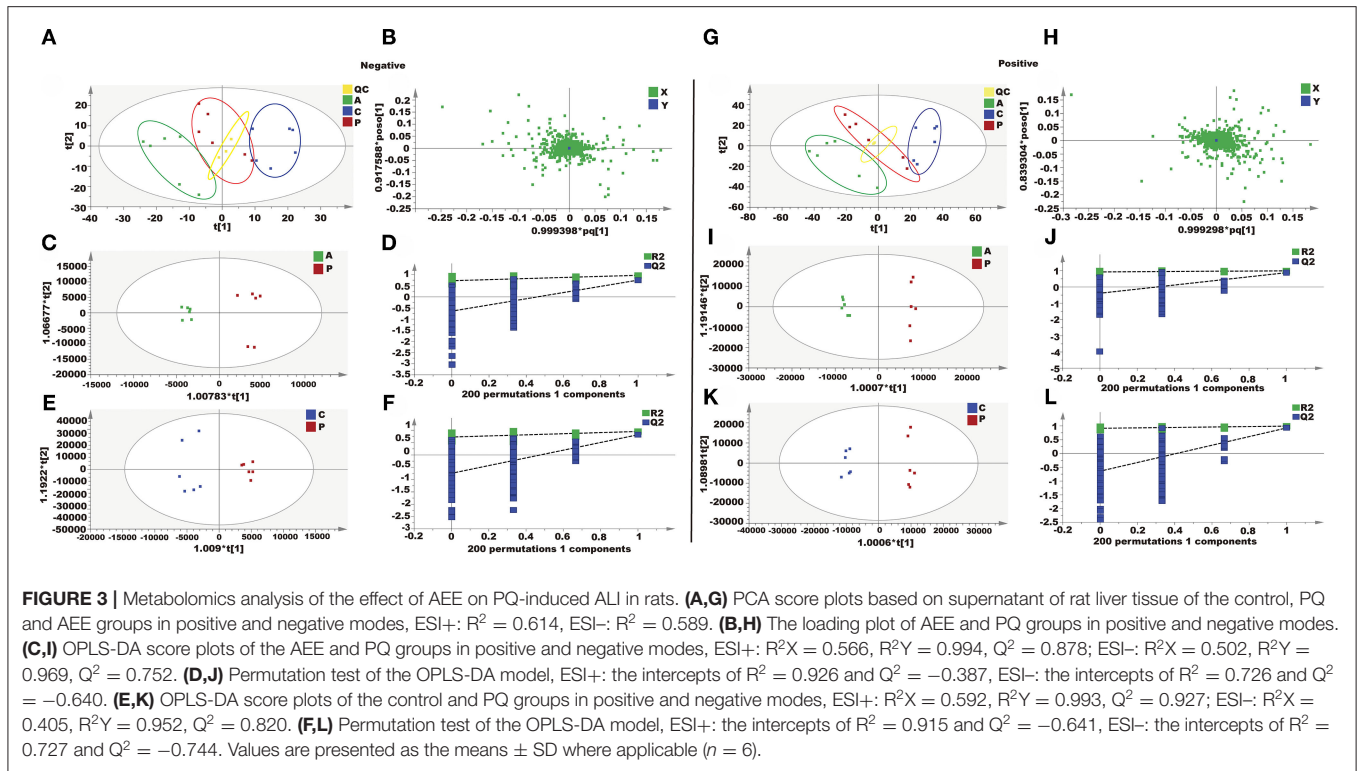
metabolism, primary bile acid biosynthesis, aminoacyl-tRNA biosynthesis, phenylalanine metabolism, histidine metabolism, pantothenate and CoA biosynthesis, ether lipid metabolism, beta-Alanine metabolism, lysine degradation, cysteine and methionine metabolism. As shown in **Figure 4**, there are significant differences in metabolic pathways, including Methylhistidine Metabolism, Bile Acid Biosynthesis, Purine Metabolism, Pantothenate and CoA Biosynthesis, Mitochondrial Beta-Oxidation of Short (*p* < 0.05). The influence of the path is mainly concentrated in Phenylalanine, tyrosine and tryptophan biosynthesis, Purine metabolism, Glycerophospholipid metabolism, and Primary bile acid biosynthesis. PQ-induced ALI in rats is mainly reflected in redox reaction and energy metabolism. The results showed that ALI induced by PQ caused metabolic disorder in rats, and AEE could effectively regulate this imbalance.

As shown in **Table 1**, AEE could increase the levels of L-Histidine, D-Asparagine, and L-Phenylalanine compared with PQ group. Some studies have shown that L-Histidine

and D-Asparagine have the effect of anti-apoptosis (31–33). The deficiency of L-Histidine can cause apoptosis through mitochondrial dysfunction, and as a substrate of asparagine biosynthesis, the deficiency of D-asparagine can also promote apoptosis (31, 32). Interestingly, higher concentrations of L-Phenylalanine also inhibited mitochondrial function and cause apoptosis (33). It is necessary to detect the expression of mitochondrial apoptosis-related proteins.

AEE Decreased the Level of Apoptosis-Related Proteins in Rat Liver Tissue Induced by PQ

To delineate the effector pathways of PQ-induced apoptosis, we examined the expression of mitochondrial apoptosis-related proteins and the expression of caspases, the central executioners of cell apoptosis. Compared with the control group, the expression of Caspase-3, Caspase-9, Bax, Cyt C, and AIF in the model group increased, while the expression



of Bcl-2 decreased (Figure 5). In AEE pretreatment group, AEE could inhibit the increase of Caspase-3, Caspase-9, Bax, Cyt C, and AIF induced by PQ, and enhance the expression of Bcl-2. Western blotting analysis showed that AEE reduced the apoptosis of liver cells via inhibiting the expression of apoptosis-related proteins in rat liver tissue induced by PQ.

DISCUSSION

AEE is synthesized by combining aspirin with eugenol based on the prodrug principal (21). As a new potential compound with anti-inflammatory and antioxidant stress pharmacological activities, AEE plays an active role in many aspects (18–21, 23, 34–38). AEE can prevent tail thrombosis induced by c kappa-carrageenan in rats (19). At the same time, AEE can attenuate thrombus induced with high-fat diet in rats by regulating platelet aggregation, hemorheology, TXB2/6-keto-PGF1 α , and blood biochemistry (38). With further study, a rat model of blood stasis was established and it was observed that AEE could alleviate the symptoms of blood stasis in rats (39). It was also found that AEE can inhibit agonist-induced platelet aggregation in rats by regulating PI3K/Akt, MAPK, and Sirt1/CD40L signal pathways (35). AEE has not only the effects of anti-inflammation, anti-thrombosis and anti-blood stasis, but also the effect of anti-atherosclerosis and other cardiovascular diseases. AEE can reduce the oxidative stress of human umbilical vein endothelial cells induced by H₂O₂ through

mitochondrial-lysosomal axis and Nrf2 signaling pathway, and then reduce the oxidative damage of vascular endothelial cells (18, 23).

PQ poisoning is caused by the selective accumulation of PQ molecules that can cause multiple organ failure and can cause severe damage to the liver (15). Although progress has been made in the comprehensive treatment of PQ poisoning, the mortality rate remains high due to the lack of effective treatment (40, 41). The underlying mechanism of PQ poisoning has not been fully elucidated, but it may be multifactorial. Studies have shown that an important cause of PQ poisoning is the excessive production of ROS (42). The overproduction of reactive oxygen species could cause excessive oxidative stress and oxidant injury in cells (43, 44). ALT and AST are enzymes found in hepatocytes. When the liver cell membrane lipid peroxidation occurs, two enzymes are easily released into the blood. The elevated levels of AST and ALT in liver and serum may indicate PQ-induced ALI. MDA is the end product of lipid peroxidation and its level can be used to assess the extent of damage from peroxidative damage (45–47). Downregulation of AST, ALT, and MDA levels meant that AEE could reduce lipid peroxidation damage. Antioxidant enzymes such as SOD, CAT and GSH-Px play an important role in ROS removal. SOD is the most important antioxidant enzyme for removing H₂O₂ from O₂⁻ (48–50). CAT and GSH-Px are the major enzymes that convert H₂O₂ to O₂ and H₂O (51–54). In the model group, ROS produced by PQ increased MDA levels and decreased SOD, GSH-Px, and CAT levels. After

TABLE 1 | Statistics of differential metabolites in the rat liver.

No	RT	VIP	Formula	Metabolites	SM	m/z	Fold Change	
							PQ/C	AEE/PQ
1	1.036	1.08	C ₆ H ₉ N ₃ O ₂	L-Histidine	ESI+	155.1546	0.86	1.03
2	1.146	2.51	C ₆ H ₁₁ NO ₂	Pipecolic acid	ESI+	129.157	0.78	1.16*
3	1.154	1.06	C ₈ H ₂₀ NO ₆ P	Glycerophosphocholine	ESI+	257.223	1.34	0.74*
4	1.213	3.14	C ₄ H ₇ NO ₃	Acetylglucine	ESI+	117.1033	0.77	1.63*
5	1.314	1.05	C ₆ H ₁₃ NO	N-(2-Methylpropyl)acetamide	ESI+	115.1735	1.04	1.47*
6	1.817	2.46	C ₄ H ₈ N ₂ O ₃	D-Asparagine	ESI+	132.1179	0.92	1.55*
7	3.638	1.17	C ₅ H ₄ N ₄ O	Hypoxanthine	ESI+	136.1115	1.37	0.92*
8	3.646	1.09	C ₁₀ H ₁₂ N ₄ O ₅	Inosine	ESI+	268.2261	0.85	1.15*
9	4.517	2.84	C ₁₀ H ₁₂ N ₄ O ₆	Xanthosine	ESI+	284.2255	0.98	1.85*
10	4.627	4.61	C ₉ H ₁₁ NO ₂	L-Phenylalanine	ESI+	165.1891	0.46	1.48*
11	4.779	2.43	C ₁₃ H ₁₇ N ₂ O ₃	Melatonin radical	ESI+	249.2857	0.39	0.75*
12	4.959	1.73	C ₁₁ H ₁₉ N ₃ O ₆	Ophthalmic acid	ESI+	289.2851	0.40	0.85*
13	5.379	1.24	C ₁₄ H ₂₈ O ₂	Nonyl isovalerate	ESI+	228.3709	0.91	0.80
14	5.717	1.42	C ₁₁ H ₂₁ N ₅ O ₅	Glutamylarginine	ESI+	303.319	0.49	0.98*
15	5.802	1.26	C ₁₁ H ₂₀ N ₂ O ₅	Glutamylleucine	ESI+	260.29	0.91	0.64
16	6.368	1.57	C ₆ H ₁₁ NO ₂	Pipecolic acid	ESI+	129.157	1.47	1.04*
17	6.682	1.07	C ₃₀ H ₄₇ N ₃ O ₁₀ S	S-(PGJ2)-glutathione	ESI+	641.773	0.65	1.19*
18	9.368	1.04	C ₁₅ H ₂₉ NO ₄	L-Octanoylcarnitine	ESI+	287.3951	0.60	2.18*
19	9.419	1.46	C ₂₄ H ₅₀ NO ₆ P	LysoPC(P-16:0)	ESI+	479.6307	1.80	3.18*
20	10.117	1.06	C ₆ H ₁₃ N ₃ O ₃	Argininic acid	ESI+	175.1857	0.79	1.78*
21	13.354	2.48	C ₂₆ H ₄₃ NO ₅	Deoxycholic acid glycine conjugate	ESI+	449.6233	0.85	0.82
22	13.969	2.42	C ₁₃ H ₂₅ NO ₃	N-Undecanoylglycine	ESI+	243.3425	0.89	1.07
23	4.995	3.96	C ₂₁ H ₃₅ N ₇ O ₁₃ P ₂ S	Dephospho-CoA	ESI-	687.15	1.95	1.04*
24	9.331	5.39	C ₂₆ H ₄₅ NO ₆ S	Taurochenodesoxycholic acid	ESI-	499.3	1.44	0.89*
25	10.677	1.07	C ₂₂ H ₄₄ NO ₇ P	LysoPC(14:1)	ESI-	465.561	2.15	1.04*
26	10.776	3.14	C ₂₆ H ₄₃ NO ₅	Chenodeoxyglycocholic acid	ESI-	449.6233	1.97	2.33
27	11.221	2.03	C ₄₇ H ₈₉ O ₈ P	PA(22:2)	ESI-	813.195	1.29	1.11
28	12.143	2.50	C ₂₄ H ₄₀ O ₅	Cholic acid	ESI-	408.5714	2.05	0.82*
29	14.502	1.11	C ₃₀ H ₃₇ NO ₈	5,9,11-trihydroxyprosta-6E,14Z-dien-1-oate	ESI-	539.625	1.29	0.77*
30	14.897	1.61	C ₂₃ H ₄₄ NO ₇ P	LysoPE(18:2)	ESI-	477.5717	1.33	0.92*
31	14.973	1.15	C ₂₅ H ₄₄ NO ₇ P	LysoPE(20:4)	ESI-	501.5931	2.06	0.75*
32	15.650	1.69	C ₂₁ H ₄₄ NO ₇ P	LysoPE(16:0)	ESI-	453.5503	1.65	1.01*

RT, retention time; VIP, variable importance in the projection; SM, scan mode; +, metabolites identified in positive mode; -, metabolites identified in negative mode. Metabolites identified in both positive and negative modes; **p* < 0.05 compared with the PQ group; C/PQ, control group compared with the PQ group; AEE/PQ, AEE group compared with the PQ group.

AEE administration, SOD, GSH-Px, and CAT increased. This indicates that AEE could restore ALI in PQ-induced rats via ROS scavenging.

Arginine synthesis and the metabolism of arginine and proline involved in L-arginine may be one of the most important metabolic pathways in which AEE plays a protective role in PQ-induced lung injury. L-arginine is a semi-essential amino acid needed for cell proliferation, and is the substrate of arginase 1 (Arg-1) and inducible nitric oxide synthase (iNOS), which is involved in the oxidative stress of the body to external stimuli. Metabonomic results showed that the biosynthesis pathway of L-arginine was inhibited in PQ group. L-arginine is a scavenger of free radicals in the body (55). L-arginine increases the activity of antioxidant enzymes and reduces the content of MDA by promoting the production

of nitric oxide (NO), thus reducing the tissue damage caused by oxidative stress (56). After pretreatment with AEE, the production of L-arginine increased, which in turn promoted the increase of SOD, GSH-Px and CAT. It is suggested that AEE may alleviate PQ-induced lung injury in rats by scavenging excessive ROS.

Glycerophospholipid metabolites, including PC and LysoPE are key components of the lipid bilayer of cells, as well as being involved in metabolism and signaling (57–59). A previous study suggested that various PCs and LysoPEs were significantly increased in rat acute blood stasis model and AEE could significantly inhibit the increase of PC and LysoPE (39). AEE increased high-density lipoprotein cholesterol serum level and decreased low-density lipoprotein cholesterol serum level in hyperlipidemia model induced by high-fat diet. Notably, the

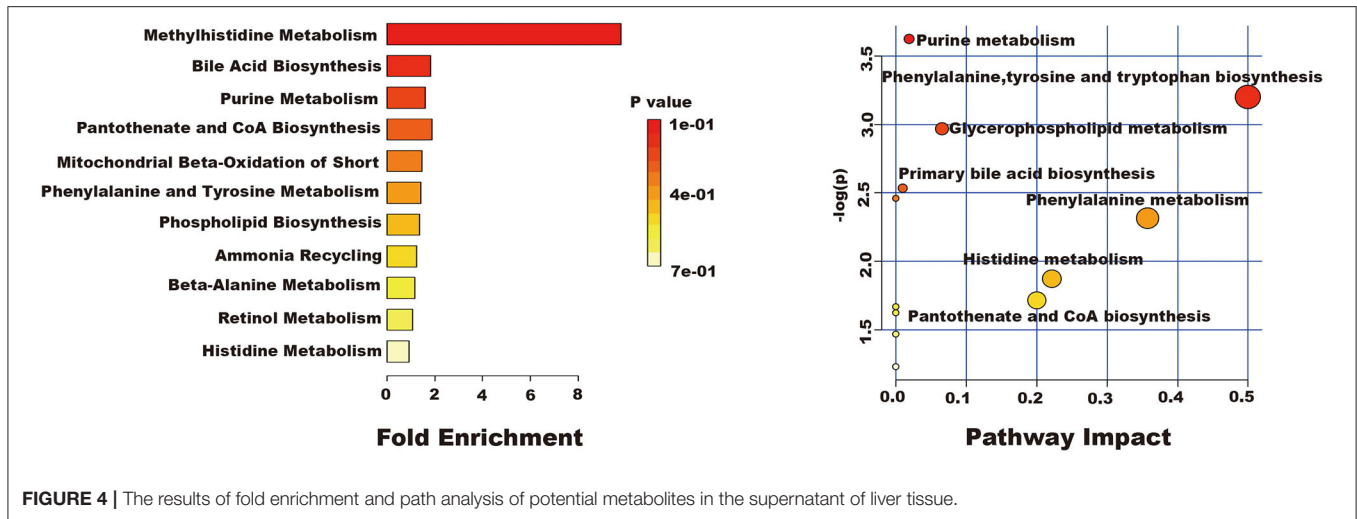


FIGURE 4 | The results of fold enrichment and path analysis of potential metabolites in the supernatant of liver tissue.

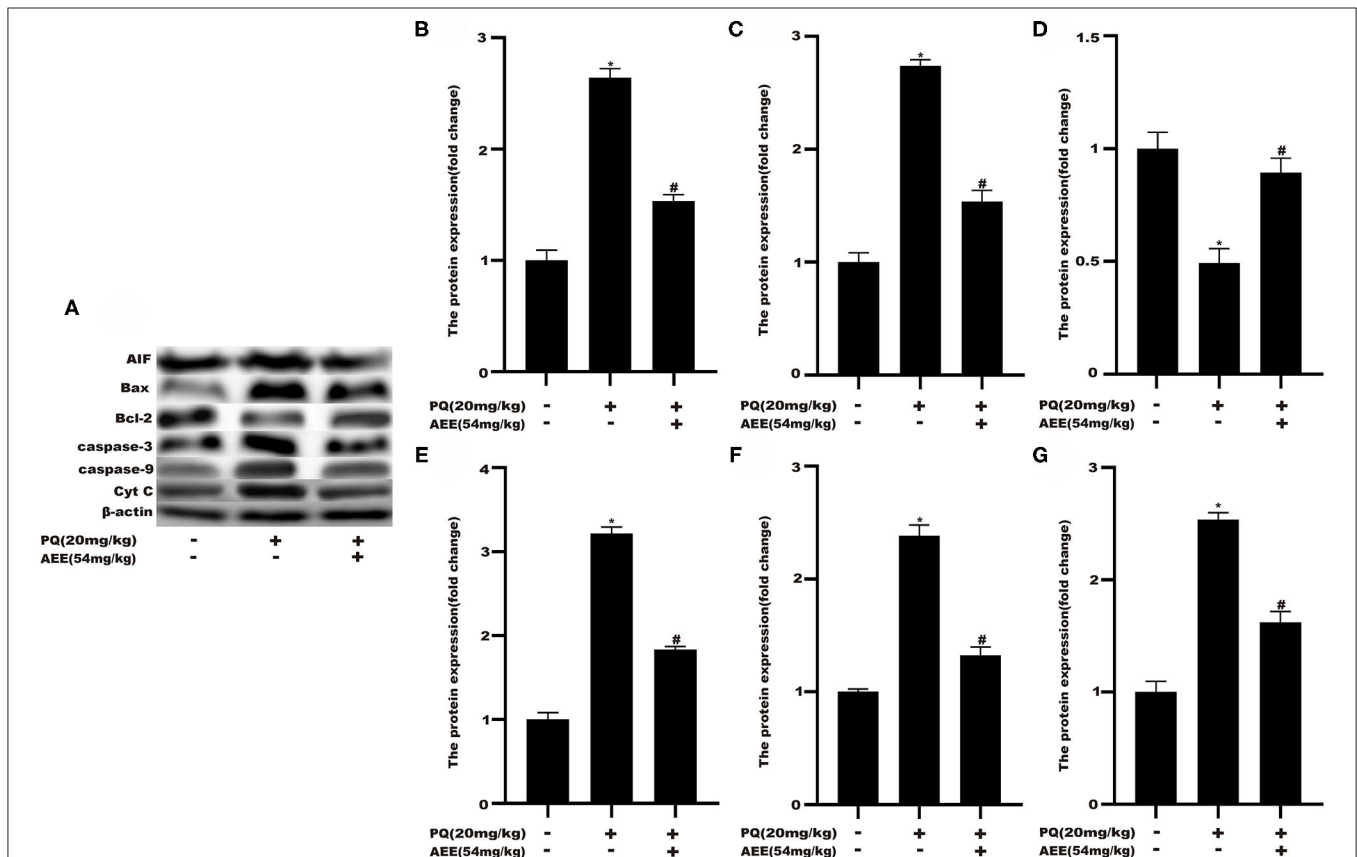
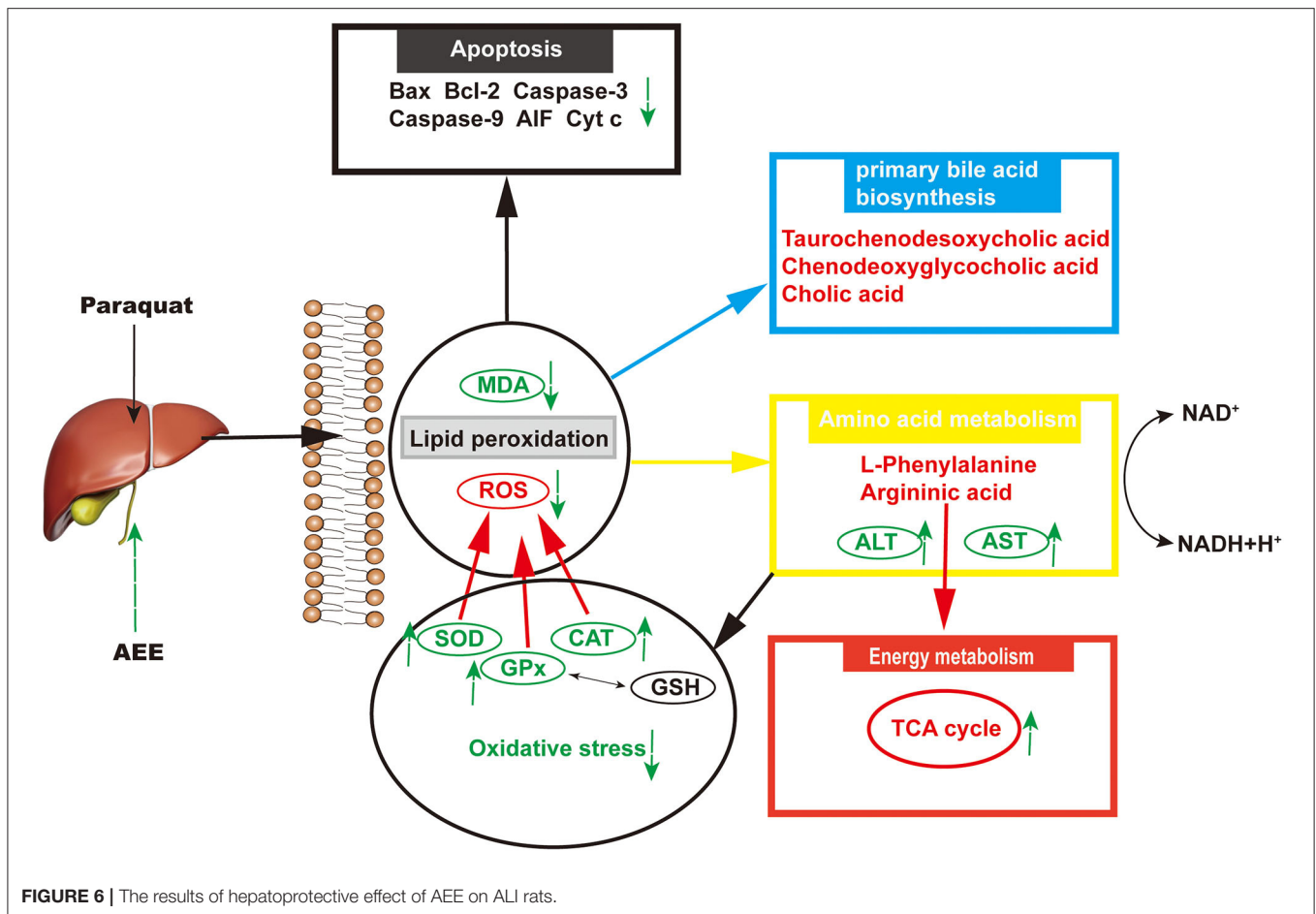


FIGURE 5 | AEE decreased the level of apoptosis-related proteins in rat liver tissue induced by PQ. **(A,B)** The expression of AIF protein in liver tissue of different treatment groups was detected. **(A,C)** The expression of Bax protein in liver tissue of different treatment groups was detected. **(A,D)** The expression of Bcl-2 protein in liver tissue of different treatment groups was detected. **(A,E)** The expression of Caspase-3 protein in liver tissue of different treatment groups was detected. **(A,F)** The expression of Caspase-9 protein in liver tissue of different treatment groups was detected. **(A,G)** The expression of Cyt C protein in liver tissue of different treatment groups was detected. Values are presented as the means \pm SD where applicable ($n = 6$). * $p < 0.05$ compared with the control group; # $p < 0.05$ compared with the PQ group.

elevated TG and TC serum levels were also reversed by AEE. All of the above implied that lipid metabolism was partly restored by AEE.

Mitochondrial damage was present due to impaired energy, amino acid, and fatty acid metabolism. The production of ROS can also cause mitochondrial apoptosis (60–62). Therefore,



apoptosis may play an important role in the pathogenesis of liver injury. In this study, the hepatic apoptotic cell rate was increased in the model group. The low percentage of hepatic apoptotic cells in the AEE group suggests that AEE enhanced antioxidant activity and attenuated apoptosis. On the other hand, the results of Western blotting analysis suggest that the expression levels of Caspase-9, Bax, Cyt C, Caspase-3, and AIF were decreased, whereas that of Bcl-2 was increased in the AEE group. **Figure 6** summarizes the protective effects of AEE on ALI rats. As shown in **Figure 6**, PQ could induce excessive production of ROS in liver tissue. Excessive ROS could further increase the excessive production of MDA and decrease the activities of antioxidant enzymes such as SOD, CAT, and GSH-Px. The decrease of antioxidant enzyme activity would lead to the release of apoptotic proteins, including Caspase-9, Bax, Cyt C, Caspase-3, and AIF. There is no doubt that when apoptosis occurs, the energy supply of mitochondria in the cell will be insufficient, and the synthesis and metabolism of some amino acids will be hindered. In this study, the metabolism and synthesis of chenodeoxycholic acid, chenodeoxycholic acid, and cholic acid were affected to some extent. Undoubtedly, during the amino acid metabolism process, the levels of L-Phenylalanine and Argininic acid decreased significantly after PQ treatment. The metabolism of amino acids would

further affect the energy metabolism of cells, especially in the TCA cycle.

CONCLUSION

AEE exhibited protective effects on PQ-induced ALI. The underlying mechanism was correlated with antioxidants that regulate amino acid, phospholipid and energy metabolism metabolic pathway disorders and alleviate liver mitochondria apoptosis.

DATA AVAILABILITY STATEMENT

The original contributions presented in the study are included in the article/supplementary materials, further inquiries can be directed to the corresponding author/s.

ETHICS STATEMENT

The animal study was reviewed and approved by the Institutional Animal Care and Use Committee of Lanzhou Institute of Husbandry and Pharmaceutical Science of Chinese Academy

of Agricultural Sciences (Approval No. NKMYD201907018; Approval Date: 18 July 2019).

AUTHOR CONTRIBUTIONS

Z-DZ designed and performed the experiments. Y-JY synthesized and purified AEE. X-WL, S-HL, and ZQ assisted with the

animal experiments. J-YL supervised the study and revised the manuscript.

FUNDING

This study was supported by grants from the National Natural Science Foundation of China (No. 31872518).

REFERENCES

- Shao Y, Zhao Y, Zhu T, Zhang F, Chang X, Zhang Y, et al. Paraquat preferentially induces apoptosis of late stage effector lymphocyte and impairs memory immune response in mice. *Int J Environ Res Public Health*. (2019) 16:60. doi: 10.3390/ijerph16112060
- Chen HG, Yang RJ, Tang Y, Fu XY. Effects of curcumin on artery blood gas index of rats with pulmonary fibrosis caused by paraquat poisoning and the expression of Smad 4, Smurf 2, interleukin-4 and interferon-. *Exp Ther Med*. (2019) 17:3664–70. doi: 10.3892/etm.2019.7341
- Sun L, Li GQ, Yan PB, Liu Y, Li GF, Wei LQ. Prediction of outcome following paraquat poisoning by arterial lactate concentration-time data. *Exp Ther Med*. (2014) 8:652–6. doi: 10.3892/etm.2014.1773
- Chen F, Liu ZL, Li W, Li D, Yan BL. The significance of serum HMGB1 level in humans with acute paraquat poisoning. *Sci Rep*. (2019) 9:1. doi: 10.1038/s41598-019-43877-1
- Xu CW, Luo JJ, He L, Montell C, Perrimon N. Oxidative stress induces stem cell proliferation via TRPA1/RyR-mediated Ca²⁺ signaling in the *Drosophila* midgut. *Elife*. (2017) 6:40. doi: 10.7554/eLife.22441.040
- Feng MX, Li YN, Ruan WS, Lu YQ. Predictive value of the maximum serum creatinine value and growth rate in acute paraquat poisoning patients. *Sci Rep*. (2018) 8:298. doi: 10.1038/s41598-018-29800-0
- Yan B, Chen F, Xu L, Xing J, Wang X. HMGB1-TLR4-IL23-IL17A axis promotes paraquat-induced acute lung injury by mediating neutrophil infiltration in mice. *Sci Rep*. (2017) 7:597. doi: 10.1038/s41598-017-00721-8
- Han JY, Zhang ZJ, Yang SB, Wang J, Yang XL, Tan DH. Betanin attenuates paraquat-induced liver toxicity through a mitochondrial pathway. *Food Chem Toxicol*. (2014) 70:100–6. doi: 10.1016/j.fct.2014.04.038
- El-Boghady NA, Abdeltawab NF, Nooh MM. Resveratrol and montelukast alleviate paraquat-induced hepatic injury in mice: modulation of oxidative stress, inflammation, and apoptosis. *Oxid Med Cell Longev*. (2017) 2017:425. doi: 10.1155/2017/9396425
- Jung E, Kim J. Aloin inhibits muller cells swelling in a rat model of thioacetamide-induced hepatic retinopathy. *Molecules*. (2018) 23:6. doi: 10.3390/molecules23112806
- Zhang L, Wang X, Chen S, Wang S, Tu Z, Zhang G, et al. Medium-chain triglycerides attenuate liver injury in lipopolysaccharide-challenged pigs by inhibiting necroptotic and inflammatory signaling pathways. *Int J Mol Sci*. (2018) 19:97. doi: 10.3390/ijms19113697
- Parvez MK, Arbab AH, Al-Dosari MS, Al-Rehaily AJ, Alam P, Ibrahim KE, et al. Protective effect of *Atriplex suberecta* extract against oxidative and apoptotic hepatotoxicity. *Exp Ther Med*. (2018) 15:3883–91. doi: 10.3892/etm.2018.5919
- Ren Y, Yang ZZ, Sun ZR, Zhang W, Chen X, Nie SN. Curcumin relieves paraquat-induced lung injury through inhibiting the thioredoxin interacting protein/NLR pyrin domain containing 3-mediated inflammatory pathway. *Mol Med Rep*. (2019) 20:5032–40. doi: 10.3892/mmr.2019.10612
- Gao C, Huang Q, Lan Q, Feng Y, Tang F, Hoi MPM, et al. A user-friendly herbicide derived from photo-responsive supramolecular vesicles. *Nat Commun*. (2018) 9:2967. doi: 10.1038/s41467-018-05437-5
- Qian JY, Deng P, Liang YD, Pang L, Wu LC, Yang LL, et al. 8-formylphlopiogonanone b antagonizes paraquat-induced hepatotoxicity by suppressing oxidative stress. *Front Pharmacol*. (2019) 10:1283. doi: 10.3389/fphar.2019.01283
- Chen D, Ma T, Liu XW, Yang C, Liu Z. Rapamycin reverses paraquat-induced acute lung injury in a rat model through inhibition of NF kappa B activation. *Int J Clin Exp Pathol*. (2015) 8:4627–38.
- Gawarammana IB, Buckley NA. Medical management of paraquat ingestion. *Br J Clin Pharmacol*. (2011) 72:745–57. doi: 10.1111/j.1365-2125.2011.04026.x
- Huang MZ, Yang YJ, Liu XW, Qin Z, Li JY. Aspirin eugenol ester attenuates oxidative injury of vascular endothelial cells by regulating NOS and Nrf2 signalling pathways. *Br J Pharmacol*. (2019) 176:906–18. doi: 10.1111/bph.14592
- Ma N, Liu XW, Yang YJ, Li JY, Mohamed I, Liu GR, et al. Preventive effect of aspirin eugenol ester on thrombosis in kappa-carrageenan-induced rat tail thrombosis model. *PLoS ONE*. (2015) 10:e0133125. doi: 10.1371/journal.pone.0133125
- Ma N, Yang GZ, Liu XW, Yang YJ, Mohamed I, Liu GR, et al. Impact of aspirin eugenol ester on cyclooxygenase-1, cyclooxygenase-2, C-reactive protein, prothrombin and arachidonate 5-lipoxygenase in healthy rats. *Iran J Pharm Res*. (2017) 16:1443–51. doi: 10.22037/ijpr.2017.2119
- Li JY, Yu YG, Wang QW, Zhang JY, Yang YJ, Li B, et al. Synthesis of aspirin eugenol ester and its biological activity. *Med Chem Res*. (2012) 21:995–9. doi: 10.1007/s00044-011-9609-1
- Li JY, Wang QW, Yu YG, Yang YJ, Niu JR, Zhou XZ, et al. Anti-inflammatory effects of aspirin eugenol ester and the potential mechanism. *Chin J Pharm Toxicol*. (2011) 25:57–61. doi: 10.3867/j.issn.1000-3002.2011.01.011
- Huang MZ, Yang YJ, Liu XW, Qin Z, Li JY. Aspirin eugenol ester reduces H2O2-induced oxidative stress of HUVECs via mitochondria-lysosome axis. *Oxid Med Cell Longev*. (2019) 2019:8098135. doi: 10.1155/2019/8098135
- Abate M, Festa A, Falco M, Lombardi A, Luce A, Grimaldi A, et al. Mitochondria as playmakers of apoptosis, autophagy and senescence. *Semin Cell Dev Biol*. (2020) 98:139–53. doi: 10.1016/j.semcdb.2019.05.022
- Hasnat M, Yuan Z, Ullah A, Naveed M, Raza F, Ashraf Baig MME, et al. Mitochondria-dependent apoptosis in triptolide-induced hepatotoxicity is associated with the Drp1 activation. *Toxicol Mech Methods*. (2019) 2019:1–10. doi: 10.1080/15376516.2019.1669247
- Meng LQ, Wang Y, Luo YH, Piao XJ, Liu C, Wang Y, et al. Quinalizarin induces apoptosis through reactive oxygen species (ROS)-mediated mitogen-activated protein kinase (MAPK) and signal transducer and activator of transcription 3 (STAT3) signaling pathways in colorectal cancer cells. *Med Sci Monit*. (2018) 24:3710–9. doi: 10.12659/MSM.907163
- Moradzadeh M, Hosseini A, Rakhshandeh H, Aghaei A, Sadeghnia HR. *Cuscuta campestris* induces apoptosis by increasing reactive oxygen species generation in human leukemic cells. *Avicenna J Phytomed*. (2018) 8:237–45.
- Tan D, Wang Y, Bai B, Yang X, Han J. Betanin attenuates oxidative stress and inflammatory reaction in kidney of paraquat-treated rat. *Food Chem Toxicol*. (2015) 78:141–6. doi: 10.1016/j.fct.2015.01.018
- Li GP, Yang H, Zong SB, Liu Q, Li L, Xu ZL, et al. Diterpene ginkgolides meglumine injection protects against paraquat-induced lung injury and pulmonary fibrosis in rats. *Biomed Pharmacother*. (2018) 99:746–54. doi: 10.1016/j.biopha.2018.01.135
- Javad-Mousavi SA, Hemmati AA, Mehrzadi S, Hosseinzadeh A, Houshmand G, Rashidi Nooshabadi MR, et al. Protective effect of *Berberis vulgaris* fruit extract against Paraquat-induced pulmonary fibrosis in rats. *Biomed Pharmacother*. (2016) 81:329–36. doi: 10.1016/j.biopha.2016.04.027
- Gwinn DM, Lee AG, Briones-Martin-Del-Campo M, Conn CS, Simpson DR, Scott AI, et al. Oncogenic KRAS regulates amino acid homeostasis and asparagine biosynthesis via ATF4 and alters sensitivity to L-asparaginase. *Cancer Cell*. (2018) 33:91–107.e106. doi: 10.1016/j.ccell.2017.12.003

32. Zhang J, Fan J, Venneti S, Cross JR, Takagi T, Bhinder B, et al. Asparagine plays a critical role in regulating cellular adaptation to glutamine depletion. *Mol Cell*. (2014) 56:205–18. doi: 10.1016/j.molcel.2014.08.018
33. Chen S, Sun M, Zhao X, Yang Z, Liu W, Cao J, et al. Neuroprotection of hydroxysafflor yellow A in experimental cerebral ischemia/reperfusion injury via metabolic inhibition of phenylalanine and mitochondrial biogenesis. *Mol Med Rep*. (2019) 19:3009–20. doi: 10.3892/mmr.2019.9959
34. Li J, Yu Y, Yang Y, Liu X, Zhang J, Li B, et al. A 15-day oral dose toxicity study of aspirin eugenol ester in Wistar rats. *Food Chem Toxicol*. (2012) 50:1980–5. doi: 10.1016/j.fct.2012.03.080
35. Shen DS, Yang YJ, Kong XJ, Ma N, Liu XW, Li SH, et al. Aspirin eugenol ester inhibits agonist-induced platelet aggregation *in vitro* by regulating PI3K/Akt, MAPK and Sirt 1/CD40L pathways. *Eur J Pharmacol*. (2019) 852:1–13. doi: 10.1016/j.ejphar.2019.02.032
36. Ma N, Liu XW, Kong XJ, Li SH, Jiao ZH, Qin Z, et al. Aspirin eugenol ester regulates cecal contents metabolomic profile and microbiota in an animal model of hyperlipidemia. *BMC Vet Res*. (2018) 14:405. doi: 10.1186/s12917-018-1711-x
37. Huang MZ, Lu XR, Yang YJ, Liu XW, Qin Z, Li JY. Cellular metabolomics reveal the mechanism underlying the anti-atherosclerotic effects of aspirin eugenol ester on vascular endothelial dysfunction. *Int J Mol Sci*. (2019) 20:165. doi: 10.3390/ijms2013165
38. Ma N, Liu XW, Yang YJ, Shen DS, Zhao XL, Mohamed I, et al. Evaluation on antithrombotic effect of aspirin eugenol ester from the view of platelet aggregation, hemorheology, TXB2/6-keto-PGF1 α and blood biochemistry in rat model. *BMC Vet Res*. (2016) 12:108. doi: 10.1186/s12917-016-0738-0
39. Shen D, Ma N, Yang Y, Liu X, Qin Z, Li S, et al. UPLC-Q-TOF/MS-based plasma metabolomics to evaluate the effects of aspirin eugenol ester on blood stasis in rats. *Molecules*. (2019) 24:80. doi: 10.3390/molecules24132380
40. Hu S, Qiao C, Yuan Z, Li M, Ye J, Ma H, et al. Therapy with high-dose long-term antioxidant free radicals for severe paraquat poisoning: A pilot study. *Exp Ther Med*. (2018) 16:5149–55. doi: 10.3892/etm.2018.6823
41. Gu SY, Yeh TY, Lin SY, Peng FC. Unfractionated bone marrow cells attenuate paraquat-induced glomerular injury and acute renal failure by modulating the inflammatory response. *Sci Rep*. (2016) 6:23287. doi: 10.1038/srep23287
42. Sun S, Wang H, Zhao G, An Y, Guo Y, Du L, et al. Complement inhibition alleviates paraquat-induced acute lung injury. *Am J Respir Cell Mol Biol*. (2011) 45:834–42. doi: 10.1165/rcmb.2010-0444OC
43. Wang Y, Wu Y, Quadri F, Prox JD, Guo L. Cytotoxicity of ZnO nanowire arrays on excitable cells. *Nanomaterials*. (2017) 7:80. doi: 10.3390/nano7040080
44. Kumar M, Padula MP, Davey P, Pernice M, Jiang Z, Sablok G, et al. Proteome analysis reveals extensive light stress-response reprogramming in the seagrass *Zostera muelleri* (Alismatales, Zosteraceae) metabolism. *Front Plant Sci*. (2016) 7:2023. doi: 10.3389/fpls.2016.02023
45. Yue QM, Peng Y, Zhao Y, Lu RX, Fu QY, Chen Y, et al. Dual-targeting for brain-specific drug delivery: synthesis and biological evaluation. *Drug Del*. (2018) 25:426–434. doi: 10.1080/10717544.2018.1431978
46. Yang BY, Zhang XY, Guan SW, Hua ZC. Protective effect of procyanidin B2 against CCl4-induced acute liver injury in mice. *Molecules*. (2015) 20:12250–65. doi: 10.3390/molecules200712250
47. Ali A, Guo D, Mahar A, Ma F, Li RH, Shen F, et al. *Streptomyces pactum* assisted phytoremediation in Zn/Pb smelter contaminated soil of Feng County and its impact on enzymatic activities. *Sci Rep*. (2017) 7:87. doi: 10.1038/srep46087
48. Wang YP, Yang L, Chen X, Ye TT, Zhong B, Liu RJ, et al. Major latex protein-like protein 43 (MLP43) functions as a positive regulator during abscisic acid responses and confers drought tolerance in *Arabidopsis thaliana*. *J Exp Botany*. (2016) 67:421–34. doi: 10.1093/jxb/erv477
49. Liu ZH, Shi XY, Li S, Zhang LL, Song XY. Oxidative stress and aberrant programmed cell death are associated with pollen abortion in isonuclear alloplasmic male-sterile wheat. *Front Plant Sci*. (2018) 9:595. doi: 10.3389/fpls.2018.00595
50. Huang CP, Qin NN, Sun L, Yu MY, Hu WZ, Qi ZY. Selenium improves physiological parameters and alleviates oxidative stress in strawberry seedlings under low-temperature stress. *Int J Mol Sci*. (2018) 19:1913. doi: 10.3390/ijms19071913
51. Belhadj S, Hentati O, Hamdaoui G, Fakhreddine K, Maillard E, Dal S, et al. Beneficial effect of jojoba seed extracts on hyperglycemia-induced oxidative stress in Rinm5f beta cells. *Nutrients*. (2018) 10:384. doi: 10.3390/nu10030384
52. Yang GY, Zhang CL, Liu XC, Qian G, Deng DQ. Effects of cigarette smoke extracts on the growth and senescence of skin fibroblasts *in vitro*. *Int J Biol Sci*. (2013) 9:613–23. doi: 10.7150/ijbs.6162
53. Volpato GT, Damasceno DC, Sinzato YK, Ribeiro VM, Rudge MVC, Calderon IMP. Oxidative stress status and placental implications in diabetic rats undergoing swimming exercise after embryonic implantation. *Reprod Sci*. (2015) 22:602–8. doi: 10.1177/1933719114556485
54. Etani R, Kataoka T, Kanzaki N, Sakoda A, Tanaka H, Ishimori Y, et al. Protective effects of hot spring water drinking and radon inhalation on ethanol-induced gastric mucosal injury in mice. *J Rad Res*. (2017) 58:614–25. doi: 10.1093/jrr/rrx021
55. Roder P, Hille C. Local tissue manipulation via a force- and pressure-controlled AFM micropipette for analysis of cellular processes. *Sci Rep*. (2018) 8:9. doi: 10.1038/s41598-018-24255-9
56. Liu YN, Paterson M, Baumgardt SL, Irwin MG, Xia ZY, Bosnjak ZJ, et al. Vascular endothelial growth factor regulation of endothelial nitric oxide synthase phosphorylation is involved in isoflurane cardiac preconditioning. *Cardiovasc Res*. (2019) 115:168–78. doi: 10.1093/cvr/cvy157
57. Jiang P, Zhang X, Huang Y, Cheng N, Ma Y. Hepatotoxicity induced by *Sophora flavescens* and hepatic accumulation of kurarinone, a major hepatotoxic constituent of *Sophora flavescens* in rats. *Molecules*. (2017) 22:809. doi: 10.3390/molecules22111809
58. Xu J, Casas-Ferreira AM, Ma Y, Sen A, Kim M, Proitsis P, et al. Lipidomics comparing DCD and DBD liver allografts uncovers lysophospholipids elevated in recipients undergoing early allograft dysfunction. *Sci Rep*. (2015) 5:17737. doi: 10.1038/srep17737
59. Srivastava NK, Sharma S, Sharma R, Sinha N, Mandal SK, Sharma D. Metabolic fingerprinting of joint tissue of collagen-induced arthritis (CIA) rat: *In vitro*, high resolution NMR (nuclear magnetic resonance) spectroscopy based analysis. *EXCLI J*. (2018) 17:257–72. doi: 10.17179/excli2017-938
60. Jiang XS, Chen XM, Wan JM, Gui HB, Ruan XZ, Du XG. Autophagy protects against palmitic acid-induced apoptosis in podocytes *in vitro*. *Sci Rep*. (2017) 7:64. doi: 10.1038/srep42764
61. Qin JL, Shen WY, Chen ZF, Zhao LF, Qin QP, Yu YC, et al. Oxoaporphine metal complexes (Co-II, Ni-II, Zn-II) with high antitumor activity by inducing mitochondria-mediated apoptosis and S-phase arrest in HepG2. *Sci Rep*. (2017) 7:56. doi: 10.1038/srep46056
62. Winckelmans E, Nawrot TS, Tsamou M, Den Hond E, Baeyens W, Kleinjans J, et al. Transcriptome-wide analyses indicate mitochondrial responses to particulate air pollution exposure. *Environ Health*. (2017) 16:7. doi: 10.1186/s12940-017-0292-7

Conflict of Interest: The authors declare that the research was conducted in the absence of any commercial or financial relationships that could be construed as a potential conflict of interest.

Copyright © 2020 Zhang, Yang, Liu, Qin, Li and Li. This is an open-access article distributed under the terms of the Creative Commons Attribution License (CC BY). The use, distribution or reproduction in other forums is permitted, provided the original author(s) and the copyright owner(s) are credited and that the original publication in this journal is cited, in accordance with accepted academic practice. No use, distribution or reproduction is permitted which does not comply with these terms.